sciendo

*Polish Journal of Chemical Technology, 21, **4**, 72—81, 10.2478/pjct-2019-0042*

Comparative studies on the adsorption of Pb(II) ions by fly ash and slag obtained from CFBC technology

Tomasz Kalak*, Ryszard Cierpiszewski

Poznań University of Economics and Business, Department of Industrial Products and Packaging Quality, Institute of Quality Science, Al. Niepodległości 10, 61-875 Poznań, Poland
**Corresponding author: e-mail: tomasz.kalak@ue.poznan.pl*

Fly ash and slag were examined for the removal processes of Pb(II) ions from water in batch experiments under different conditions of adsorbent dosage, initial concentration, pH and contact time. The materials are industrial waste generated from the high temperature treatment of sewage sludge by the circulating fluidized bed combustion (CFBC) technology. Physical and chemical properties, as well as adsorption efficiency and calculated maximum adsorption capacity of Pb(II) ions were determined using a variety of methods. The kinetic analysis revealed that the adsorption process is better described by the pseudo-second order equation and it is well fitted to the Freundlich model.

Keywords: fly ash, slag, adsorption of lead ions, isotherms, kinetics.

INTRODUCTION

Rapid industrialization and economic development contribute to the continuous introduction of heavy metals into the natural environment. In accordance with World Health Organization (WHO), Cd, Cr, Cu, Pb, Hg and Ni are the most toxic metals[1]. These days it is still an ecological problem around the world[2]. They are generated during industrial processing and introduced into the natural environment, and thereby enter the food chain and become a health problem. They do not decompose and have a tendency to bioaccumulate in living organisms, causing various diseases, disorders and even death[3]. According to the Agency for Toxic Substances and Disease Registry, lead is ranked second because of the highest toxicity among all substances[4]. Taking the hazards of lead into account, various methods should be developed to remove it from sewage.

There are many ways of wastewater treatment, such as chemical precipitation, coagulation, ion exchange, electrochemical methods, photocatalytic degradation and others[5]. Among them, adsorption seems to be an alternative, promising and cost effective method. Silica gels, ion exchange resins, activated carbon, zeolites, mesoporous materials, silicoaluminate minerals or graphene oxides are popular adsorbents used in the process due to their high recovery efficiency[6]. Nevertheless, their high costs are a negative side. Nowadays, alternative and cheaper adsorbents are mainly sought among waste generated as a result of industrial processing, including fruit and vegetable residues, biomass, waste from wood industry (e.g. hardwood), waste from agriculture (e.g. corn straw, carrot, rape), oil shale ash, lignin, coal gangue, slag, fly ash and others[5–8].

In accordance with Central Statistical Office in Poland, there was about 540.3 thousand tons of municipal sewage sludge produced by waste treatment plants in 2013[9]. In the European Union it is estimated that about 10 million tons of dry matter of sewage sludge is produced every year and there is an upward trend of around 2–2.5%[9, 10]. Many technologies are used to reduce sludge mass through thermal treatment. However, the circulating fluidized bed combustion (CFBC) technology has recently aroused an interest and is currently recommended by the European Union as the most effective. The most essential advantage is a significant reduction in sludge weight and the products of combustion processes are fly ash and slag. The materials are characterized by an irregular shape with a porous surface, no odor, large contents of minerals or a high specific surface area, due to which they find many industrial applications, including adsorption of metal ions[10–12]. Thus, thanks to the development of the CFBC technology, cheap fly ash and slag may have an enormous pro-ecological significance in the separation processes of toxic substances, such as heavy metals in the future.

The purpose of the studies was to examine the physicochemical properties of fly ash and slag generated from the combustion of sewage sludge using the circulating fluidized bed combustion (CFBC) technology by several methods, and compare their adsorption properties in relation to Pb(II) ions under different conditions of adsorbent dosage, initial concentration, pH and contact time. In addition, the adsorption kinetics, equilibrium and the Langmuir and Freundlich isotherms were described.

MATERIAL AND METHODS

Fly ash and slag preparation

The fly ash and slag used in these studies were obtained in a sewage treatment plant in Poland in the circulating fluidized bed combustion (CFBC) technology. The samples were taken from a fluidized bed reservoir and prepared in accordance with the Polish Standards PN-EN 14899:2006 and PN-EN 15002:2006. The samples were dried at a temperature of 105°C to a constant weight (<0.2% moisture content). All chemical substances were analytically pure and distilled water was used in the experiments.

Fly ash and slag characterization

Determination of granulation was carried out according to the Polish Standard PN-C-97555.01. Separation of individual fractions was performed by screening through sieves with mesh diameters of 0.212 to 1.0 mm. Separated fractions were weighed and this process was repeated

three times. The content of individual particles (grain faction, X [%]) was calculated based on the equation (1).

$$X = \frac{m_1 \times 100\%}{m_2} \quad (1)$$

where: m_1 [g] is mass of sifted fly ash or slag, m_2 [g] – initial mass of a sample.

The particle size distribution was determined by the laser diffraction method using a Zetasizer Nano ZS (Malvern Instruments Ltd., UK). Bulk density was determined in accordance with the standard PN-S-96035:1997. The mass and volume of samples was measured using a measuring cylinder in triplicate. It (X [g/cm^3]) was calculated based on the equation (2).

$$X = \frac{m_1 - m_0}{V} \quad (2)$$

where: m_1 [g] is mass of a cylinder with fly ash or slag; m_0 [g] – mass of an empty cylinder and V [cm^3] – volume of the sample in a cylinder.

In addition, the following determinations of fly ash and slag were made: 1) the elemental composition using a scanning electron microscope (SEM) Hitachi S-3700N with an attached a Noran SIX energy dispersive X-ray spectrometer (EDS) microanalyser (ultra-dry silicon drift type with resolution (FWHM) 129 eV, accelerating voltage: 20.0 kV); 2) X-ray diffraction analysis using Bruker AXS D8 Advance (Germany); 3) thermogravimetric analysis using the apparatus Setsup DTG, DTA 1200 (Setram; temperature range 30°C–600°C; the rate of temperature increase 10°C/min; gas flow rate of nitrogen 20 mL/min); 4) the specific surface area and the average pore diameter by the Brunauer, Emmett and Teller (BET) method using Autosorb iQ Station 2 (Quantachrome Instruments, USA); 5) the pore volume by Barret, Joyner and Halenda (BJH) method using Autosorb iQ Station 2 (Quantachrome Instruments, USA); 6) electrokinetic zeta potential using Zetasizer Nano ZS (Malvern Instruments Ltd., UK) equipped with autotitrator (MPT-2 Autotitrator); 7) the morphology of the samples was analyzed using a scanning electron microscope (SEM) EVO-40 (Carl Zeiss, Germany); 8) the surface structure was analyzed using a Fourier transform attenuated total reflection (FT-IR ATR) Spectrum 100 (Perkin-Elmer, Waltham, USA).

Energy dispersive spectroscopy (EDS) is a method used in scanning electron microscopy (SEM) for the determination of chemical elements in solid samples. A single EDS measurement is a result of the acquisition of energy-dispersive spectrum in which there are characteristic peaks of chemical elements. Samples of fly ash and slag were dried to a constant mass, then placed in the vacuum chamber of the apparatus prepared for measurements. Then the sample was treated with a focused electron beam with energy values up to 30 keV. Electrons hitting the surface of the sample are scattered into the material and ionize its atoms by knocking out secondary electrons from the stationary shells. The obtained gaps in the electron shell are filled with other electrons coming from the outer shells of the atom. Then, the ionized atoms emit X-ray quanta of discrete energy, which are typical for the chemical elements present in the sample material. The emitted photons are collected by the EDS detector and transmitted through an electronic system to the multi-channel analyzer, where the pulses are separated in accordance with their amplitude. The number of quanta (intensity) of X-rays is proportional to the concentration of a particular element in the sample. Finally, the energy-dispersive spectra are sent to a computer equipped with a special software system for processing spectral data. The EDS analysis is considered a non-destructive method, because there is no difference between the quality of samples before and after analysis[13].

The Pb(II) ions adsorption process

Determination of the adsorption efficiency of Pb(II) on fly ash and slag was carried out in batch experiments. Lead nitrate ($Pb(NO_3)_2$ with analytical purity (standard for AAS 1 g/L, Sigma-Aldrich (Germany)) was used in these studies. The adsorbents (20–200 mg) and a portion of $Pb(NO_3)_2$ solution (20 mL) containing 2.5–20 mg/L of Pb(II) ions at pH range 2–5 were placed in a 50 mL conical flask and shaken at 150 rpm during 1 h until equilibrium was reached. The pH of Pb(II) solutions were adjusted using 0.1 M HNO_3 and NaOH solutions. Subsequently, the contents of the flasks were centrifuged for 15 min. at 4000 rpm for phase separation. Next, the solutions above the adsorbents were analyzed by the atomic absorption spectrophotometer (F-AAS, at a wavelength λ = 217 nm for lead) SpectrAA 800 (Varian, Palo Alto, USA) to determine the Pb(II) concentrations after adsorption. The measurements were performed in triplicate at room temperature (23 ± 1°C), under environmental pressure and average results were presented. The removal efficiency A [%] and the adsorption capacity q_e [mg/g] were calculated in accordance with the equations 3 and 4, respectively:

$$A = \left[\frac{C_0 - C_e}{C_0}\right] \times 100\% \quad (3)$$

$$q_e = \frac{(C_0 - C_e) \times V}{\mathrm{m}} \quad (4)$$

where: C_0 and C_e [mg/L] are initial and equilibrium metal ion concentrations, respectively; V [L] – volume of solution and m [g] – mass of adsorbents.

Kinetics and isotherm parameters were calculated using pseudo-first-order (5) and pseudo-second-order (6), Langmuir (7) and Freundlich (8) models according to the equations, respectively:

$$q_t = q_e(1 - e^{k_1 t}) \quad (5)$$

$$q_t = \frac{q_e^2 k_2 t}{1 + q_e k_2 t} \quad (6)$$

$$q_e = \frac{q_{max} K_L C_e}{1 + K_L C_e} \quad (7)$$

$$q_e = K_F C_e^{\frac{1}{n}} \quad (8)$$

where: q_t [mg/g] is the amount of Pb(II) ions adsorbed at any time t [min.]; q_e [mg/g] – the maximum amount of Pb(II) ions adsorbed per mass of the material at equilibrium; k_1 [1/min.] – the rate constant of pseudo-first-order adsorption; k_2 [g/(mg · min.)] – the rate constant of pseudo-second-order adsorption; q_{max} (mg/g) – the maximum adsorption capacity; K_L – the Langmuir constant; C_e [mg/L] – the equilibrium concentration after

the adsorption process; K_F – the Freundlich constant and $1/n$ – the intensity of adsorption.

RESULTS AND DISCUSSION

Characteristics of the adsorbents

The determination of grain composition was carried out and the results are following: a) the particles of fly ash: 0–0.212 mm – 87.6%, 0.212–0.500 mm – 11.1%, 0.500–1.0 mm – 1.3%, b) particles of slag: 0–0.212 mm – 13.04%, 0.212–0.5 mm – 73.6%, 0.500–1.0 mm – 11.4%, 1.0–1.7 mm – 0.62%, > 1.7 mm – 1.28%. It has been revealed that the particles are not homogeneous, but their size has a significant impact on the adsorption process. Based on the literature, the smaller size of fly ash particles the greater Pb(II) adsorption efficiency, which is associated with a larger surface area and the amount of active centers[14]. Therefore, the smallest fractions, less than 0.212 mm in diameter, were applied in the experiments.

The analysis of particle size distribution had some limitations, i.e. not all particles were able to form a slurry in an aqueous solution (heavier and larger particles fell to the bottom of the solution). Therefore, it was possible to analyze only the particles suspended in the solution. Only one peak in the plot has been revealed corresponding to particle size of 1205 and 955.4 nm for fly ash and slag, respectively. The difference is due to the fact that the ash particles are more volatile and less dense compared to the slag, hence the particles with larger diameter were able to suspend.

Fly ash and slag contain particles of various shapes and sizes, which combine into agglomerations of different densities. In these studies bulk density was determined by loosely filling the samples into a cylinder and by thickening on a vibrating table. The results were equal to 0.71 ± 0.01 g/cm^3 and 1.44 ± 0.02 g/cm^3 for fly ash, respectively. In case of slag the results were estimated at 0.82 and 1.34 g/cm^3, respectively. The study exposed an increase in the bulk density after the compaction process.

The SEM-EDS method was used to analysis of the samples and the results are presented in Table 1. The peaks present in the spectra correspond to elements and oxides. Fly ash mainly contains O, Ca, P, Al, Si, Fe, Mg and CaO, P_2O_5, Al_2O_3, SiO_2, Fe_2O_3, CO_2, MgO. In addition, slag is mainly composed of Ca, O, Fe, S, P, Al, Si, C and CaO, SO_3, Fe_2O_3, P_2O_5, SiO_2, CO_2, Al_2O_3. There are also other elements and oxides in smaller amounts. The presence of oxides was calculated by stoichiometry in the EDS microanalysis based on estimation and not a measurement. Characteristically, these materials are agglomerates composed of different particles and their quantitative and qualitative composition slightly differs depending on the location of the measuring point on the sample using the SEM-EDS method. However, a comparison of the compositions of these materials with others published in the literature is presented in Table 1. There was similar content observed for oxides Na_2O, TiO_2, MnO or Fe_2O_3. Differences in the composition of other substances result from many factors, such as combustion process parameters, a type of dried sewage sludge, an analytical method, etc. Bhardwaj et al. reported that the presence a greater number of carbon black and Fe_2O_3 in fly ash composition promotes better mercury adsorption efficiency[15, 16].

Based on the thermogravimetric measurements a weight loss (TGA) is observed with an increase in temperature. In the case of fly ash there is a constant continuous and almost a linear weight loss up to 2.5%. The change may be caused by the removal of adsorbed water from the sample, as well as the removal of CO and volatile constituents (e.g. organic compounds). At a temperature of 400–450°C significant mass loss is noticed in the case of slag. This phenomenon is probably the result of the combustion of organic residues adsorbed on the sample surface[24]. Increasing the temperature to 550–600°C results in subsequent weight loss up to 0.5% in total. This change can be caused by the degradation of the surface wall of grains as a result of the release of gaseous products from their interior.

Based on the SEM-EDS analysis, the presence of carbon dioxide in fly ash and slag was observed after the fluidized bed combustion process (Table 1). It may be attributed to carbon oxidation and calcium carbonate decomposition according to the following chemical oxidation – reduction reactions:

$$C + O_2 \rightarrow CO_2 \quad (9)$$

$$CaCO_3 \rightarrow CaO + CO_2 \quad (10)$$

Carbon dioxide is produced as a result of the carbon oxidation for temperatures less than 973 K (700°C). The thermogravimetric analysis (TGA) shows a weight loss in 500–600°C range, which is also attributed to calcium carbonate decomposition into calcium oxide and carbon dioxide[25, 26].

A derivative weight loss [%/min.] is presented by the DTG analysis. Only one band is visible at 330°C (weak band, fly ash) and 410°C (more intensive band, slag). This

Table 1. The chemical composition of fly ash and slag (SEM-EDS analysis) and comparison with literature data

Elements	C	O	Na	Mg	Al	Si	P	S	K	Ca	Ti	Mn	Fe	Zn
Fly ash, weight [%]	1.85	44.8	0.54	3.28	6.41	5.51	11.3	0.41	1.11	17.7	0.54	0.23	5.43	0.87
Fly ash, atomic [%]	3.41	61.9	0.52	2.99	5.25	4.34	8.11	0.28	0.63	9.76	0.25	0.09	2.15	0.29
Slag, weight [%]	1.19	36.5	0.27	1.0	1.92	1.98	2.47	4.59	0.13	37.9	0.44	-	7.84	—
Slag, atomic [%]	2.46	56.9	0.3	1.03	1.78	1.76	1.99	3.58	0.08	23.6	0.21	—	3.51	—
Slag, ref.[17]	—	20.0	0.27	0.44	4.05	21.18	2.26	—	1.94	13.59	0.61	2.39	33.26	—
Oxides	CO_2		Na_2O	MgO	Al_2O_3	SiO_2	P_2O_5	SO_3	K_2O	CaO	TiO_2	MnO	Fe_2O_3	ZnO
Fly ash, oxides [%]	6.79		0.73	5.44	12.1	11.8	26.02	1.02	1.3	24.7	0.89	0.29	7.8	1.1
Slag, oxides [%]	4.34		0.37	1.66	3.64	4.24	5.65	11.5	0.16	53.1	0.73	-	11.2	—
Fly ash, ref.[18]	—		0.37	1.4	27.0	48.8	1.2	0.22	0.85	6.2	1.3	0.15	10.2	—
Fly ash, ref.[19]	—		0.38	1.2	23.63	—	1.31	0.28	0.84	1.74	1.32	0.13	15.3	—
Fly ash, ref.[20]	—		0.61	0.3	29.8	56.01	0.44	—	0.73	2.36	1.75	—	3.58	—
Fly ash, ref.[21]	—		0.37	0.77	26.49	53.36	1.43	0.20	0.80	1.34	1.47	—	10.86	—
Fly ash, ref.[22]	—		0.42	0.78	23.59	52.11	1.31	0.49	0.80	2.61	0.88	0.03	7.39	—
Fly ash, ref.[23]	—		—	0.97	22.03	57.25	—	0.76	0.52	2.97	0.68	—	8.36	—

probably corresponds to dehydroxylation of $Ca(OH)_2$[26]. The next DTG slope is recorded at about 600°C, which may result from the release of gaseous products. The negative values of signals can indicate the presence of endothermic reactions.

The BET analysis indicated that the specific surface area (S_{BET}) of fly ash and slag is 3.75 and 1.87 m^2/g, volume of the pores (Vp) is 0.014 and 0.0096 cm^3/g and average pore diameter (Apd) is 17.6 and 21.2 nm, respectively (Figure 1 A, B). Adsorption isotherms have different courses, which are dependent on the pore size and the intensity of the adsorbate interaction with the adsorbent. Their shape is typical of III isotherms, which are convex in the direction of the pressure axis. The shape informs about the co-operating adsorption, which means that the previously adsorbed particles can lead to increased adsorption of other remaining ones. The effect of the adsorbate – adsorbate is more important than the adsorbate – adsorbent interaction. At the low relative pressure, low adsorption efficiency appears as a result of weak adsorbate – adsorbent interactions. Nevertheless, when a molecule is adsorbed once, the interaction of the adsorbate with the adsorbate promotes the adsorption of other ions, and as a consequence the isotherm becomes convex in the direction of the pressure axis[27].

In accordance with IUPAC classification, pores occurring in fly ash and slag are classified as mesopores (2.0–50 nm)[28]. The pore volume distribution was determined by BJH method. During capillary condensation in mesopores, the pressure enhancement increases the thickness of the adsorbate layer on the pore walls. Thus, the adsorption isotherm in the range of relative pressure $0.01 < p/p_0 < 0.5$ was determined to indicate volume and distribution on the basis of mesopores[29].

Zeta potential parameter was determined, because it is important for many applications in industry, such as environmental protection or sewage treatment plants. Fig. 2 shows that fly ash and slag curve courses are quite similar, but the potential values for slag are slightly smaller. Low stability of the dispersion system is presented at pH 2.1–2.6 (5.6–18 mV). It has been revealed that pH values influence the surface charge, which exhibits a decrease from 18 mV (pH 2.17) to 1.2 mV (pH 4.2), and then it rises to 9.2 (pH 7). It is characteristic that the charge does not reach isoelectric point (IEP), because there is a larger number of negative ions than positive ones. Then the zeta potential was measured after Pb(II) ion adsorption processes. In the case the surface charge varies from positive (8–18 mV, pH 2.1) to negative (–30, –34 mV, pH 7) values. At pH 2–2.5 and 6.5–7 there is sufficient charge to confer solution stability. The isoelectric point (IEP) is reached at pH 3.5–3.7, which can be explained by the fact that the balance between positive and negative ions has been achieved, which is very important from a practical consideration (the system is least stable). In this point particles of fly ash and slag have the smallest viscosity, solubility and osmotic pressure. The adsorption process of Pb(II) ions (positively charged) is a preferred process, similarly to the fly ash and slag materials that had mostly negative surface before the adsorption. Lead ions were added in the form of $Pb(NO_3)_2$ salt to the adsorption process, which means simultaneous adding positively charged Pb(II)

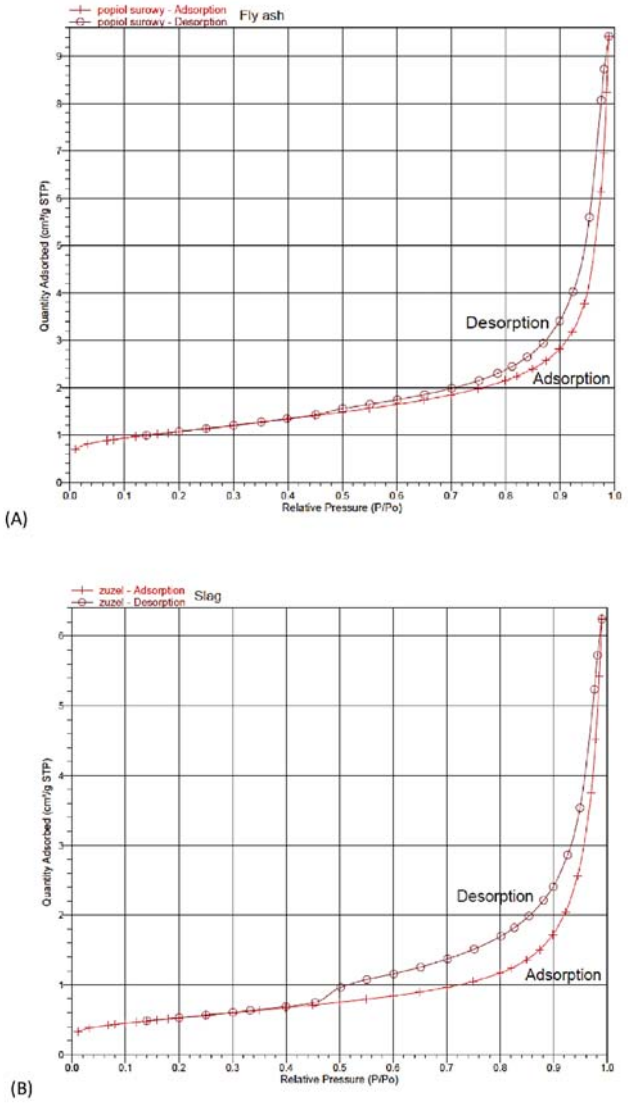

Figure 1. The low temperature BET adsorption and desorption isotherm: A) fly ash, B) slag

and negatively charged NO_3^-. The surface negative ions were neutralized by Pb(II) ions, which was recorded by lowering the zeta potential values. It has been reported that pH influences zeta potential. In acidic solutions adsorption of positively charged ions increases the zeta potential value. However, it is decreased in alkaline solutions by a greater number of negatively charged ions.

The SEM images of fly ash and slag particles before adsorption processes were analyzed and shown in Fig. 3.

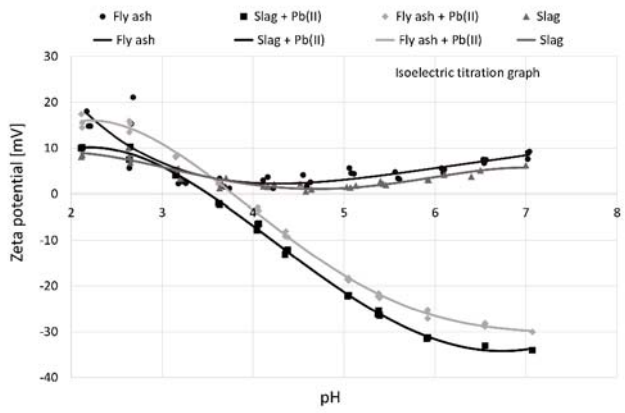

Figure 2. The change in zeta potential with equilibrium pH

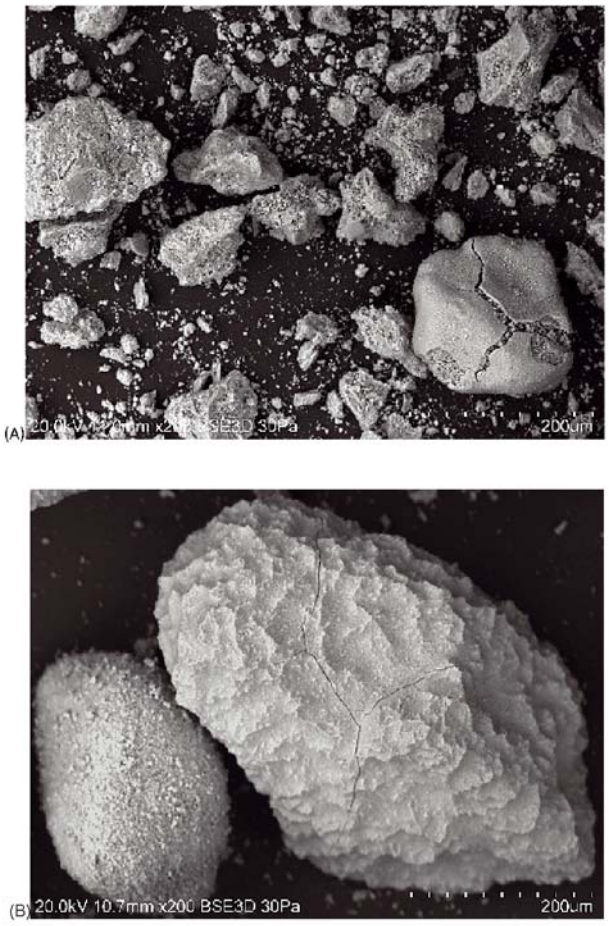

Figure 3. SEM images of fly ash (A) and slag (B) (x200)

It has been revealed that the particles are formed into irregular agglomerates and contain mesopores. They are compact and spongy with a porous surface and heterogeneous structure. The smaller particles are less irregular than larger ones. The acicular, elongated and irregular shape of particles depends on the combustion temperature in the process. The particles take on a more spherical shape or crystalline form when the time of the combustion process is longer[30].

Comparison of adsorption processes of Pb(II) ions on fly ash and slag

Effect of adsorbent dosage

The impact of adsorbent dosage on the adsorption of Pb(II) is shown in Fig. 4. The process efficiency increased with an increase in the adsorbent dosage up to 1 and 4 g/L for slag and fly ash, respectively. The doses can be considered as optimal. After that the adsorption is kept constant and does not expose any significant changes despite increasing adsorbent doses. In addition, the experimental adsorption capacity decreased from 11.1 to 0.8 mg/g and from 21 to 4.7 mg/g, respectively. With this phenomenon, active sites are fully utilized when interacting between the adsorbent and Pb(II) ions at low mass[31]. It is assumed that at higher adsorbent mass, active sites available for adsorption were not fully utilized. Thus, the decrease in adsorption capacity with an increase in adsorbent dosage was observed.

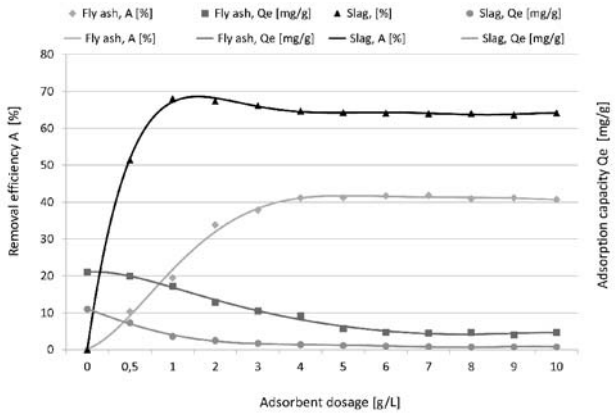

Figure 4. The impact of adsorbent dosage on adsorption of Pb(II) (the initial concentration of Pb(II) C0 = 102 mg/L; initial pH 2.0; T = 23±1°C; contact time = 60 min.)

Effect of initial concentration

The impact of the initial concentration of Pb(II) ions at the adsorbent dosage of 1 and 2 g/L was presented in Fig. 5. In the case of fly ash the removal efficiency A [%] decreased and experimental adsorption capacity Q_e [mg/g] began to grow when the concentration of metal ions increased. The removal efficiency reached

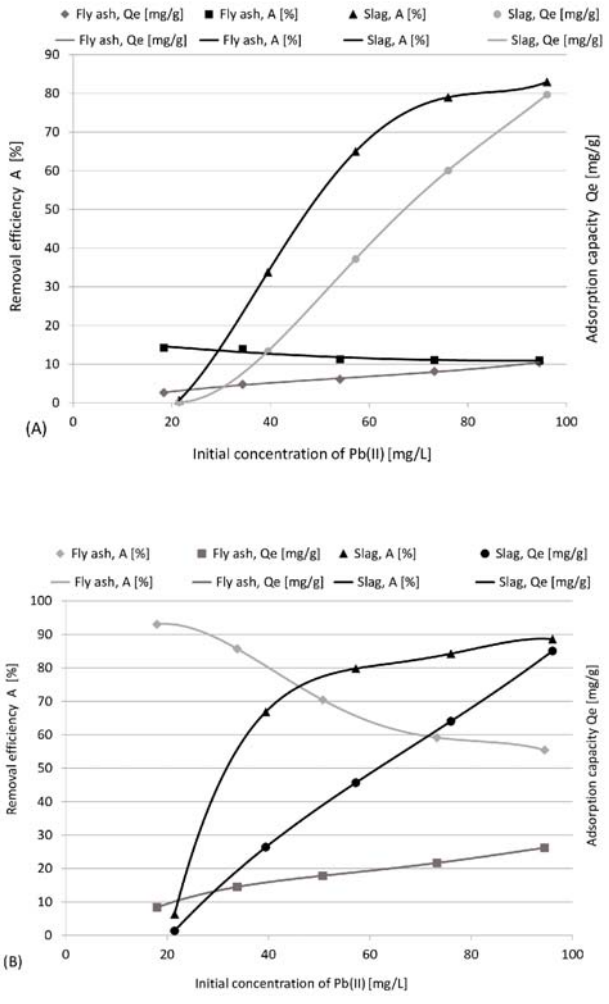

Figure 5. The impact of initial concentration on the Pb(II) adsorption (initial pH 2.0; contact time = 60 min.; T = 23±1°C) at adsorbent dosage: A) 1 g/L; equilibrium pH 3.1; B) 2 g/L; equilibrium pH 3.8

the maximum in case of applying 2 g/L fly ash (93%). In comparison, it has been revealed that slag curves maintained an upward trend in both cases. When the metal concentration of 100 mg/L was applied, the removal efficiency was equal to 83% and 88.6% for 1 and 2 g/L, respectively. In this case increasing Pb(II) concentration had a positive effect on the adsorption process. An increase in the experimental adsorption capacity occurred, because the active centers to be filled were still present and their total amount available had a huge impact on adsorption efficiency.

Effect of initial pH

The impact of initial pH on the adsorption was determined and shown in Fig. 6. The initial pH range from 2.0 to 6.2 was used based on the Pourbaix diagram for lead ions in aqueous solutions and literature review[32, 33]. In case of fly ash (1 g/L) the removal efficiency exhibits rather low values (4.5%) at initial pH 2.0 due to the competitive reaction between H^+ and Pb(II) ions to occupy active sites on the surface of the material[34]. It should be noted that the interfacial tension values at the solid-liquid interface strongly influence the adsorption processes[35]. When higher pH values were used, the adsorption of Pb(II) increased due to more favorable adsorption conditions and greater affinity to active sites. Oxides present in these materials (SiO_2, Al_2O_3, etc.) are sensitive to changes in pH, hence they were reflected in the behavior of Pb(II) ions. The proposal of ion exchange mechanism between H^+ and Pb(II) ions in the adsorption process can be presented by the equations 11–13.

$$X\text{-}OH + H_3O^+ \leftrightarrow X\text{-}OH_2^+ + H_2O \quad (11)$$

$$X\text{-}OH + OH^- \leftrightarrow X\text{-}O^- + H_2O \quad (12)$$

$$2(X\text{-}O^-) + Pb^{2+} \leftrightarrow (X\text{-}O)_2Pb \quad (13)$$

where: X can be Si, Al, Fe or another one. As the pH increased, the number of SiO^- anions (dissociated from the hydroxyl group on the surface of the material) increased, resulting in the higher electrostatic attraction between the interacting ions. While slag was used in the same adsorption conditions, the removal efficiency (75–83%) was rather stable and did not exhibit a significant change with the pH growth. The experimental adsorption capacity also showed stable course at about 13–16 mg/g. In these experimental conditions, the precipitation of Pb compounds can be taken into account because of the distribution of metal ions as a function of pH.

The studies of adsorption kinetics

Effect of contact time

The effect of contact time on the adsorption process was examined and shown in Fig. 7. A rapid increase in the first 10 minutes occurred and then an equilibrium was achieved for the adsorption of Pb(II) ions on fly ash. The best process efficiency was obtained at a dose of 5 g/L (95–97%) and can be ranked as follows: 5 > 4 > 3 > 2 > 1 g/L. In case of slag material an equilibrium was achieved after about 20–30 min. Compared to fly ash, taking the amount of applied dose into account the removal efficiency can be ranked as follows: 3 > 2 > 1 > 4 > 5 g/L. The rapid initial increase in adsorption may be due to the presence of free spots on the adsorbent surface and a high concentration gradient of Pb(II) ions at the adsorbent-solution interface. Adsorption equilibrium was gradually achieved as a result of occupying active centers by cations, therefore sorption mechanism may take other forms[36].

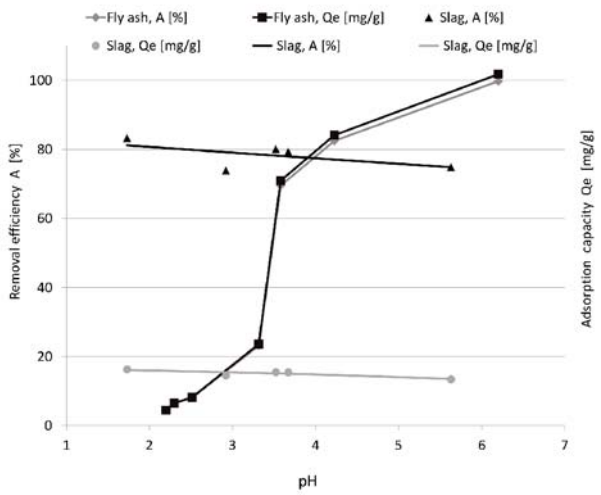

Figure 6. The impact of pH on the Pb(II) adsorption (initial concentration of Pb(II) = 102 mg/L; T = 23±1°C; contact time = 60 min.; pH range 2.0–6.2) at adsorbent dosage 1 g/L

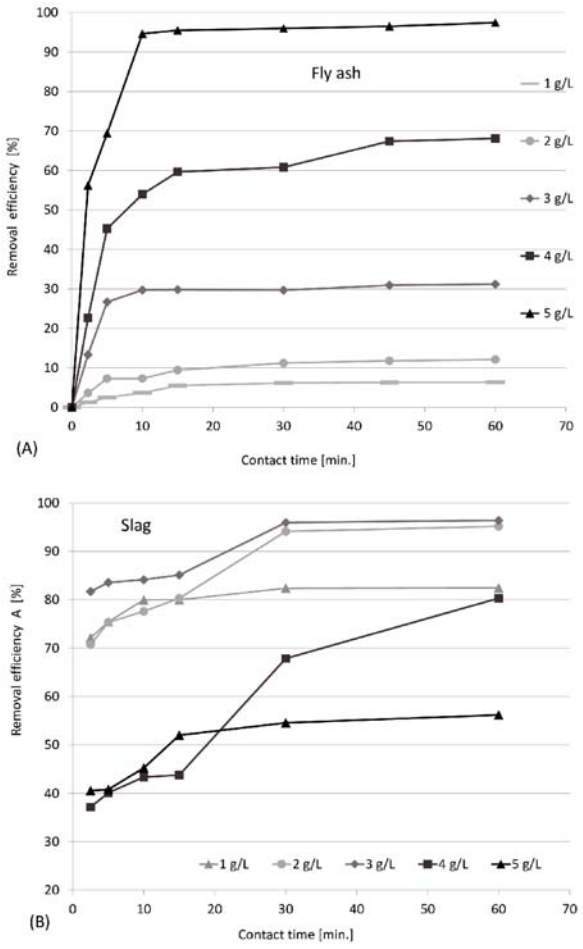

Figure 7. The impact of contact time on the Pb(II) adsorption (initial concentration of Pb(II) = 99.74 mg/L (fly ash) and 94.3 mg/L (slag); adsorbent dosage = 1–5 g/L; T = 23±1°C; initial pH 2.0

Pseudo-first-order and pseudo-second-order kinetic models

Pseudo-first-order and pseudo-second-order model were used to describe kinetics of Pb(II) adsorption on fly ash and slag (Table 2). Based on the calculation the correlation coefficients R^2 for the pseudo-first-order kinetic model were low. This indicates that the adsorption mechanism does not fit into a first-order reaction. Thus, pseudo-second-order equation was applied for subsequent studies. Adsorption rate constants k_{ad}, equilibrium adsorption densities q_e and correlation coefficients R^2 were shown in Table 2 for comparison. According to the data, higher correlation coefficients for both adsorbents were noticed in the pseudo-second-order model, so there is a higher degree of correlation between the calculated q_t and the experimental q_e values. To conclude, the pseudo-second-order model best fits the description of adsorption kinetics of Pb(II) ions on fly ash and slag. Therefore, the process seems to be diffuse and chemisorption probably occurs on the material surface[37]. There is a likelihood that chemical bonds were formed during the adsorption process and adhesion to the material surface occurred. There is a smaller probability of particle collision in case of lower concentration of Pb(II) ions in the solution. Furthermore, lead ions could join ash and slag active centers more quickly[38].

Adsorption isotherms

The Langmuir and Freundlich isotherm models were used to describe the adsorption process. As it is seen in Table 3 the isotherm parameters generally fit into the Langmuir equation for 1 g/L and 2 g/L of fly ash and slag, respectively. The values of calculated q_m and constant K_L are estimated at around 48–52 mg/g and 0.03–0.2, respectively. The K_L is related to the adsorbent and solute binding energy, which refers to the spontaneity of the adsorption process. If the K_L value is greater, the spontaneity of the adsorption reaction is higher. As a result, it is associated with a more stable product and more efficient adsorption capacity[39].

The Freundlich isotherm model is an empirical equation and refers to the relationship between the concentration of Pb(II) ions adsorbed per unit mass of adsorbent (q_e) and their concentration in the solution at equilibrium (C_e)[40]. The constant K_f is responsible for the adsorption capacity of adsorbents and the slope *1/n* relates to the influence of concentration on the adsorption capacity. In this study the Freundlich constants K_f and n are estimated at around 0.97–8.6 and 1.97–1.5 for fly ash, 1.4–1.9 and 1.4–1.6 for slag, respectively. In accordance with the results present in Table 3 the data is more closely in line with the Freundlich model. The greater K_f value, the higher amount of adsorbent dosage. Therefore, based on the constants values it can be stated that it is easy to separate Pb(II) ions from aqueous solutions.

The SEM – EDS analysis of fly ash and slag

The morphology and composition of adsorbents after adsorption of Pb(II) were analyzed using scanning electron microscopy combined with electron dispersive spectroscopy (SEM–EDS) (Figure 8, Table 4). An analysis of SEM images showed that fly ash and slag particles before and after adsorption keep the original shape. The spectra analysis showed that the concentration of elements and oxides depends on the type of fly ash and slag particle, and is always slightly different due to the position of the measurement point on the surface of particles. Therefore, the particles are not homogeneous due to their quantitative composition, but the presence of individual elements is virtually the same. When the results of EDS analysis before and after adsorption process were compared (Tables 1 and 4), it was revealed that the amount of some elements in the samples decreased. This means that in all probability some of them in the ionic form (such as C, O, Mg, Al, Si, P, Na, K, Ca, Ti, Fe) were transferred into an aqueous solution. In addition, the EDS analysis confirmed the presence of adsorbed lead ions on the surface of fly ash and slag samples after the adsorption process.

The Pb(II) distribution on the surface of the analysed samples was determined by SEM-EDS mapping using the backscattered detector (Fig. 9). The results show a homogeneous distribution of the element in the analyzed fly ash sample and that the Pb signal is intensive.

Table 2. A comparison of the kinetic parameters of pseudo-first-order and the pseudo-second-order rate equations

Adsorbent dosage [g/L]		Pseudo-first-order kinetic model			Pseudo-second-order kinetic model		
		k_{ad} [min^{-1}]	q_e [mg/g]	R^2	k [g/mg min]	q_e [mg/g]	R^2
Fly ash	1	0.044	11.24	0.867	0.106	6.696	0.963
	2	0.109	4.79	0.950	0.141	5.82	0.962
	3	0.442	9.92	0.895	0.049	9.84	0.999
	4	0.196	14.08	0.996	0.0197	15.62	0.996
	5	0.343	19.159	0.847	0.0121	19.05	0.995
Slag	1	0.162	32.1	0.686	0.00078	78.12	0.999
	2	0.095	23.06	0.596	0.003	38.03	0.999
	3	0.059	19.2	0.456	0.003	39.4	0.998
	4	0.04	14.7	0.641	0.04	10.98	0.998
	5	0.03	12.7	0.202	0.05	9.74	0.950

Table 3. Isotherm model parameters for adsorption of Pb(II) onto fly ash and slag

Adsorbent dosage [g/L]		Langmuir isotherm			Freundlich isotherm		
		Calculated q_m [mg/g]	K_L [L/mg]	R^2	K_f [mg/g] [L/mg]$^{(1/n)}$	n	R^2
Fly ash	1	48.35	0.0369	0.964	0.974	1.967	0.989
	2	51.98	0.2019	0.971	8.595	1.549	0.985
Slag	1	54.08	0.1408	0.554	2.358	1.038	0.623
	2	43.76	0.1367	0.650	3.180	1.169	0.549

Ribeiro et al. presented similar results of EDS analysis concerning distribution of several metals on the surface of anthracite fly ash[41].

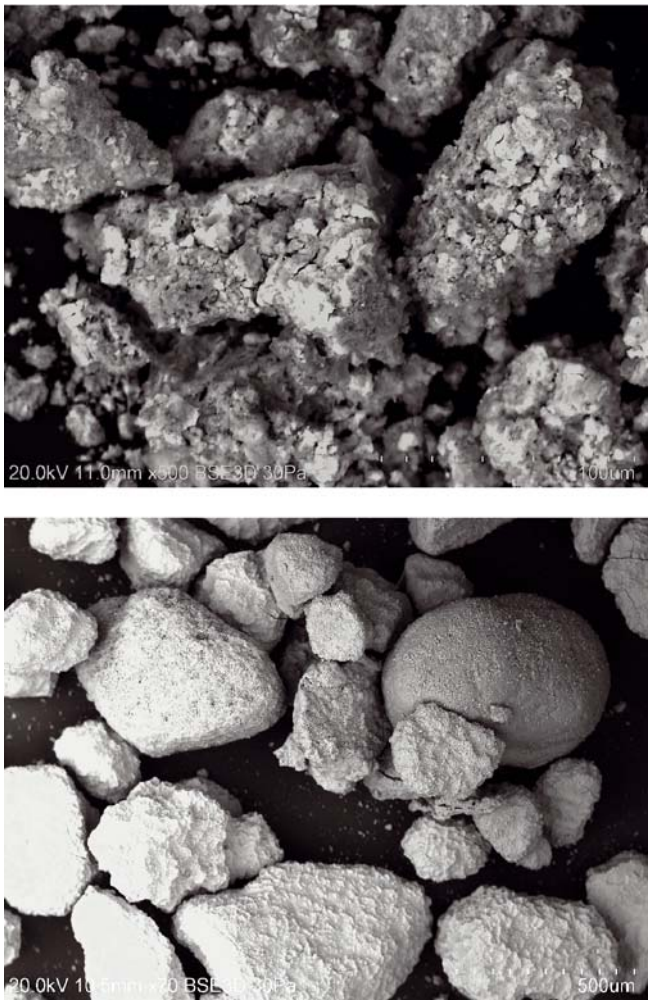

Figure 8. The SEM image of fly ash (A, x200) and slag (B, x200) after Pb(II) adsorption

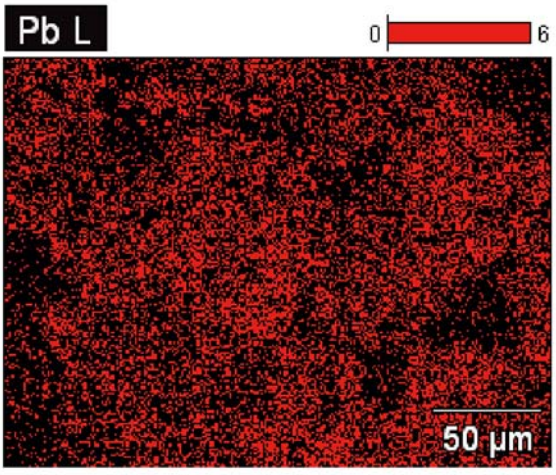

Figure 9. The SEM – EDS mapping image of the distribution and relative proportion (intensity) of Pb element over the scanned area of fly ash (magn. x500)

FT-IR analysis

The FT-IR analysis of fly ash and slag before and after Pb(II) ions adsorption processes was conducted (Figs. 10, 11, Table 5). In case of fly ash (Fig. 10) intensity of peaks increased after Pb(II) adsorption and additionally their position changed. The peak at 3643 cm^{-1} disappeared, but the bands at around 3253 cm^{-1} and 1740 cm^{-1} appeared. The bands at 1026 cm^{-1} and 800–400 cm^{-1} became strongly intensive due to a possible complexation process or formation of surface complexes with Pb(II) ions. In case of slag (Fig. 11) a change in intensity of peaks also was observed at 1408, 1112, 874, 713 and 600–380 cm^{-1} because of a possible occurrence of bonds with lead ions (Pb–O). The strong band at 1112 cm^{-1} moved slightly towards the lower wavelength values. Additionally, the EDS analysis revealed the presence of lead oxides.

Table 5. FT-IR peaks of fly ash and slag and their assignment

FT-IR band [cm^{-1}]	Assignment (vibrations, species)
3642, 3643	asymmetric and symmetric stretching vibrations O–H (probably amorphous silicates or hydrated aluminum silicates)
3253, 3268	stretching vibrations O–H
1740	stretching vibration of C=O bonds of saturated aliphatic aldehyde, carboxylic acid or its ester[42]
1408, 1424	valence vibration of carbonate ions
1026, 1112, 1095	asymmetric stretching vibrations of silica Si–O–Si and Al–O–Si
873,874	symmetric stretching of Al–O–M[42], vibration of carbonates (calcite)
713	symmetric stretching of Si–O–Si and Al–O–Si[42]
677, 676	stretching vibrations Al–O[42]
611, 609, 592	stretching vibrations Al–O[42]
596	vibrations Si-O-Pb
546, 553	O-P-O, O=P-O bending vibration (probably P_2O_5)
457, 437, 432, 414, 415, 403, 390	bond bending vibrations Si-O-Si[43]

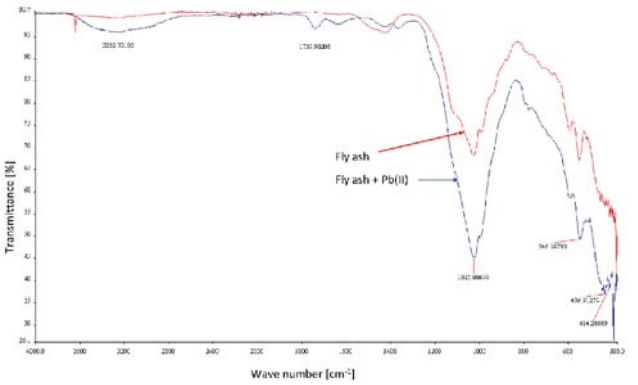

Figure 10. FT-IR spectrum of fly ash before and after Pb(II) ions adsorption

Table 4. The chemical composition after adsorption of Pb(II) ions (determined by EDS microanalyser)

Elements	C	O	Mg	Al	Si	P	K	Ca	Ti	Fe	Zn	Pb
Fly ash, weight [%]	1.22	33.29	0.52	5.35	5.24	6.28	1.08	6.69	1.23	11.09	1.28	26.75
Fly ash, atomic [%]	3.03	61.95	0.63	5.9	5.56	6.04	0.82	4.97	0.76	5.91	0.58	3.84
Slag, weight [%]	0.56	28.99	0.21	0.86	1.71	1.24	0.1	32.89	0.41	9.21	—	23.82
Slag, atomic [%]	2.08	57.4	0.37	1.76	1.85	1.67	1.06	22.81	0.25	4.88	—	5.87
Oxides	CO_2		MgO	Al_2O_3	SiO_2	P_2O_5	K_2O	CaO	TiO_2	Fe_2O_3	ZnO	PbO
Fly ash, oxides [%]	4.48		0.86	10.1	11.21	14.39	1.3	9.36	2.05	15.86	1.59	28.81
Slag, oxides [%]	3.04		1.24	2.63	3.82	4.54	0.16	45.2	0.51	13.1	—	25.76

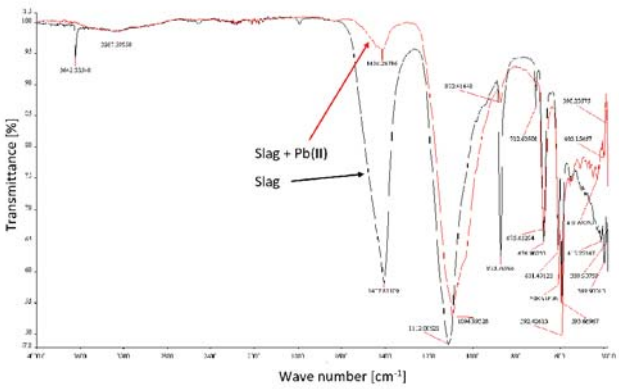

Figure 11. FT-IR spectrum of slag before and after Pb(II) ions adsorption

CONCLUSIONS

In these studies, fly ash and slag generated in one of the municipal wastewater treatment plants in Poland using the circulating fluidized bed combustion (CFBC) technology were examined for the possibility of removing lead ions from aqueous solutions in adsorption processes. Firstly, the adsorbents characteristics were described by the use of a variety of analytical methods. Next, the impact of adsorbent dosage, initial concentration, pH and contact time on Pb(II) ions adsorption efficiency were examined. A maximum adsorption efficiency of 97.4% and 96.4%, and the calculated maximum adsorption capacity of 51.98 mg/g and 54.08 mg/g for fly ash and slag were achieved, respectively. Equilibrium and adsorption kinetics were studied and characteristic parameters for isotherms were calculated and analyzed. In accordance with the kinetic data, the pseudo-second-order kinetic model and the Freundlich model suited better these adsorption processes.

To conclude, these studies revealed that low-cost fly ash and slag obtained in the CFBC technology can be successfully used to adsorb lead ions from aqueous solutions due to the highly-mineral composition and appropriate physicochemical properties. Therefore, this achievement creates new perspectives for the use of the waste materials obtained from the effective technology for removing metals from municipal and industrial effluents.

ACKNOWLEDGEMENTS

This research did not receive a specific grant from any a funding agency in the public, commercial or not-for-profit sectors.

LITERATURE CITED

1. WHO (2006), In: *Guidelines for Drinking-water Quality*, Vol. 1. WHO Library Cataloguing-in-Publication Data, Geneva.

2. Kalak, T. & Strus, B. (2014). Influence of Selected Surfactants and High-Octane Oxygen Components on Water Content, Electrolytic Conductivity in Gasoline, and Interfacial Tension in the Water/Gasoline System. *Energy&Fuels.* 28, 1926−1939. DOI: 10.1021/ef4018338.

3. Wani, A.L., Ara, A. & Usmani, J.A. (2015). Lead toxicity: a review. *Interdiscip. toxicol*. 8, 55–64. DOI: 10.1515/intox-2015-0009.

4. ATSDR's Substance Priority List (2017), The Agency for Toxic Substances and Disease Registry (ATSDR).

5. Azimi, A., Azari, A., Rezakazemi, M. & Ansarpour, M. (2017). Removal of Heavy Metals from Industrial Wastewaters: A Review. *ChemBioEng Reviews.* 4, 1–24. DOI: 10.1002/cben.201600010.

6. Young, R.T. (2003). Adsorbents: fundamentals and applications. John Wiley & Sons, Inc., Hoboken, New Jersey, USA, ISBN 0-471-29741-0.

7. Kalak, T., Dudczak, J. & Cierpiszewski, R. (2015). Adsorption behaviour of copper ions on elderberry, gooseberry and paprika waste from aqueous solutions. *Proceedings of 12th International Interdisciplinary Meeting on Bioanalysis (CECE)*, Brno, Czech Republic, 123–127.

8. Kalak, T. & Cierpiszewski, R. (2018). Adsorptive removal of copper and cadmium ions using fly ash resulting from CFBC technology. *Proceedings of 15th International Interdisciplinary Meeting on Bioanalysis (CECE)*, Brno, Czech Republic, 177–181.

9. Environmental Protection 2014. Statistical Yearbook of GUS, Warsaw, 2014.

10. Milieu Ltd, WRc, RPA and DG Environment (2008). Environmental, Economic and Social Impacts of the Use of Sewage Sludge on Land. *Final report for the European Commission*.

11. AKPGO, Update National Waste Management Plan 2014, Warsaw, 2015.

12. Nowak, B., Aschenbrenner, P. & Winter, F. (2013). Heavy metal removal from sewage sludge ash and municipal solid waste fly ash – A comparison. *Fuel Process. Technol.* 105, 195–201. DOI: 10.1016/j.fuproc.2011.06.027.

13. Wassilkowska, A., Czaplicka-Kotas, A., Bielski, A., Zielina, M. (2014). An analysis of the elemental composition of micro-samples using EDS technique. *Tech. Trans.* 18, 133–148. DOI: 10.4467/2353737XCT.14.283.3371.

14. Itskosa, G., Koukouzasa, N., Vasilatosb, C., Megremib, I. & Moutsatsouc, A. (2010). Comparative uptake study of toxic elements from aqueous media by the different particle-size fractions of fly ash. *J. Hazard. Mater.* 183, 787–792. DOI: 10.1016/j.jhazmat.2010.07.095.

15. Yadla, S.V., Sridevi, V. & Chandana Lakshmi, M.V.V. (2012). Adsorption Performance Of Fly Ash For The Removal Of Lead. *Int. J. Eng. Res. Technol.* 1, 1–7. ISSN: 2278-0181.

16. Bhardwaj, R., Chen, X. & Vidic, R.D. (2009). Impact of fly ash composition on mercury speciation in simulated flue gas. *J. Air Waste Manage. Assoc.* 59(11), 1331–1338. DOI: 10.3155/1047-3289.59.11.1331.

17. Thiele, A., Török, B. & Költő, L. (2012). Energy dispersive X-ray analysis (SEM-EDS) on slag samples from medievalbloomery workshops – the role of phosphorus in the archaeometallurgy of iron in Somogy County, Hungary, *Proceedings of the 39th International Symposium for Archaeometry*, Leuven, 1–9.

18. Kong, D.L.Y., Sanjayan, J.G. & Sagoe-Crentsil, K. (2007). Comparative performance of geopolymers made with metakaolin and fly ash after exposure to elevated temperatures. *Cem. Concr. Res*. 37, 1583–1589. DOI: 10.1016/j.cemconres.2007.08.021.

19. Temuujin, J., & Riessen, A.V. (2009). Effect of fly ash preliminary calcination on the properties of geopolymer. *J. Hazard. Mater.* 164, 634-639. DOI: 10.1016/j.jhazmat.2008.08.065.

20. Thokchom, S., Ghosh, P. and Ghosh, S. (2009). Resistance of Fly Ash Based Geopolymer Mortars in Sulfuric Acid. *ARPN J. Eng. Appl. Sci.* 4, 65–70. ISSN 1819-6608.

21. Hardjito, D., Wallah, S.E., Sumajouw, D.M.J. & Rangan, B.V. (2005). Fly ash-based geopolymer concrete. *Aust. J. Struct. Eng.* 6, 77–86. DOI: 10.9790/1684-1404071216.

22. Mustafa, A.M., Kamarudin, H., Omar Karem, A.K.A., Ruzaidi, C.M., Rafiza, A.R. & Norazian, M.N. (2011). Optimization Of Alkaline Activator/Fly Ash Ratio On The Compressive Strength Of Manufacturing Fly Ash-Based Geopolymer. *2nd International Conference on Mechanical, Industrial, and Manufacturing Technologies (MIMT 2011)*, Singapore.

23. Alinnor, I.J. (2007). Adsorption of heavy metal ions from aqueous solution by fly ash, *Fuel*. 86, 853–857.

24. Bieniek. J., Ściubidło, A. & Izabela Majchrzak-Kucęba, I. (2013). Properties of fly ash derived from coal combustion in air and in oxygen enriched atmosphere in a pilot plant installation Oxy-Fuel CFB 0,1 MW, *Energetyka* 11/2013 (713), 821–826. ISSN 0013-7294.

25. Paya, J., Monzo, J., Borrachero, M.V., Perris, E. & Amahjour, F. (1998). Thermogravimetric methods for determinig carbon content in fly ashes, *Cem. Concr. Res.* 28(5), 675–686. DOI: 10.1016/S0008-8846(98)00030-1.

26. Mohebbi, M., Rajabipour, F. & Scheetz, B.E. (2015). Reliability of Loss on Ignition (LOI) Test for Determining the Unburned Carbon Content in Fly Ash. *World of Coal Ash (WOCA) Conference in Nasvhill*.

27. Bansal, R.C. & Goyal, M. (2005). *Activated Carbon Adsorption*. CRC Press, Taylor and Francis Group, LLC, Boca Raton, FL. DOI: 10.1201/9781420028812.

28. Sing, K.S.W. (1982). Reporting Physisorption Data for Gas/Solid Systems with Special Reference to the Determination of Surface Area and Porosity. *Pure Appl. Chem.* 54, 2201–2218. DOI: 10.1351/pac198254112201.

29. Liu, J., Qiu, Q., Xing, F. & Pan, D. (2014). Permeation Properties and Pore Structure of Surface Layer of Fly Ash Concrete. *Mater.* 7, 4282–4296. DOI: 10.3390/ma7064282.

30. Ho, YS. (2005). Effect of pH on lead removal from water using tree fern as the sorbent. *Bioresour Technol.* 96(11): 1292–1296. DOI: 10.1016/j.biortech.2004.10.011.

31. Paliulis, D. & Bubėnaitė, J. (2014). Effect of pH for lead removal from polluted water applying peat. The 9th International Conference „Environmental Engineering 2014". DOI: 10.3846/enviro.2014.042.

32. Weng, C.H. & Huang, C.P. (2004). Adsorption characteristics of Zn(II) from dilute aqueous solution by fly ash. *Colloid Surf. A*. 247, 137–143. DOI: 10.1016/j.colsurfa.2004.08.050.

33. Adebowale, K.O., Unuabonah, I.E. & Olu-Owolabi, B.I. (2006). The effect of some operating variables on the adsorption of lead and cadmium ions on kaolinite clay. *J. Hazard. Mater.* 134, 130–139. DOI: 10.1016/j.jhazmat.2005.10.056.

34. Sari, A., Tuzen, M. & Citak, D. (2007). Equilibrium, kinetic and thermodynamic studies of adsorption of Pb(II) from aqueous solution onto Turkish kaolinite clay. *J. Hazard. Mater.* 149, 283–291. DOI: 10.1016/j.jhazmat.2007.03.078.

35. Kalak, T. & Cierpiszewski, R. (2015). Correlation analysis between particulate soil removal and surface properties of laundry detergent solutions. *Text. Res. J.* 85, 1884–1906. DOI: 10.1177/0040517515578329.

36. Kavitha, D. & Namasivayam, C. (2007). Experimental and kinetic studies on methylene blue adsorption by coir pith carbon. *Bioresour. Technol.* 98, 14–21. DOI: 10.1016/j.biortech.2005.12.008.

37. Ho, Y.S. & McKay, G. (1999). Psudo-second order model for sorption processes, *Process Biochem.* 34, 451–465. DOI: 10.1016/S0032-9592(98)00112-5.

38. Wong, K.K., Lee, C.K., Low, K.S. & Haron, M.J. (2003). Removal of Cu(II) and Pb(II) by tartaric acid modified rice husk from aqueous solutions. *Chemosphere*. 50, 23-28. DOI: 10.1016/S0045-6535(02)00598-2.

39. Wang, S.B. & Ariyanto, E. (2007). Competitive adsorption of malachite green and Pb ions on natural zeolite. *J. Colloid Interf. Sci.* 314, 25–31. DOI: 10.1016/j.jcis.2007.05.032.

40. Kumar, P.S., Vincent, C., Kirthika, K. & Kumar, K.S. (2010). Kinetics and equilibrium studies of Pb^{2+} ion removal from aqueous solutions by use of nano-silversol-coated activated carbon. *Braz. J. Chem. Eng.* 27, 339–346. DOI: 10.1590/S0104-66322010000200012.

41. Ribeiro, J., DaBoit, K., Flores, D., Kronbauer, M.A. & Silva, L.F. (2013). Extensive FE-SEM/EDS, HR-TEM/EDS and ToF-SIMS studies of micron- to nano-particles in anthracite fly ash, *Science of the Total Environment*. 452–453C, 98–107. DOI: 10.1016/j.scitotenv.2013.02.010.

42. Ueda, S., Koyo, H., Ikeda, T., Kariya, Y. & Maeda, M. (2000). Infrared emission spectra of CaF_2-CaO-SiO_2 melt. *ISIJ Int.* 40(8), 739–743. DOI: 10.2355/isijinternational.40.739.

43. Iliashevsky, O., Rubinov, E., Yagen, Y. & Gottlieb, M. (2016). Functionalization of Silica Surface with UV-Active Molecules by Multivalent Organosilicon Spacer. *Open J. Inorg. Chem.* 6, 163–174. DOI: 10.4236/ojic.2016.63012.